Sog/Chordin is required for ventral-to-dorsal Dpp/BMP transport and head formation in a short germ insect

Maurijn van der Zee, Oliver Stockhammer, Cornelia von Levetzow, Rodrigo Nunes da Fonseca, and Siegfried Roth*

Institut für Entwicklungsbiologie, Universität zu Köln, Gyrhofstrasse 17, 50923 Cologne, Germany

Edited by Kathryn V. Anderson, Sloan–Kettering Institute, New York, NY, and approved September 7, 2006 (received for review June 20, 2006)

Bone morphogenetic protein (BMP) signaling plays a major role in dorsoventral patterning in vertebrates and in *Drosophila*. Remarkably, in *Tribolium*, a beetle with an ancestral type of insect development, early BMP/*dpp* exhibits differential expression along the anteroposterior axis. However, the BMP/Dpp inhibitor Sog/chordin is expressed ventrally and establishes a dorsal domain of BMP/Dpp activity by transporting BMPs toward the dorsal side, like in *Drosophila*. Loss of *Tribolium* Sog not only abolishes dorsoventral polarity in the ectoderm, but also leads to the complete absence of the CNS. This phenotype suggests that *sog* is the main BMP antagonist in *Tribolium*, in contrast to vertebrates and *Drosophila*, which possess redundant antagonists. Surprisingly, Sog also is required for head formation in *Tribolium*, as are the BMP antagonists in vertebrates. Thus, in *Tribolium*, the system of BMP and its antagonists is less complex than in *Drosophila* or vertebrates and combines features from both, suggesting that it might represent an ancestral state.

amnion | serosa | dorsoventral patterning | neuroectoderm | growth zone | *Tribolium castaneum*

Bone Morphogenetic Proteins (BMPs) pattern the early vertebrate embryo along the dorsoventral axis (1, 2). A ventral center in the embryo expresses BMPs and induces ventral mesoderm and nonneurogenic ectoderm. A dorsal organizer expresses BMP antagonists such as *chordin*, allowing the formation of dorsal mesoderm and neuroectoderm.

BMPs play a similar role in *Drosophila*. High BMP signaling levels are found along the dorsal midline where an extraembryonic tissue, the amnioserosa, is specified (3, 4). Moderate levels induce the dorsal ectoderm. At more ventral positions, BMP activity is inhibited by the secreted chordin-like BMP inhibitor *short gastrulation* (sog), which allows neurectoderm specification (5, 6). Thus, in both *Drosophila* and vertebrates, conserved molecular mechanisms establish an antineurogenic BMP activity gradient, albeit with opposite orientations along the dorsoventral axis. This situation has been explained by two evolutionary scenarios. The first assumes that the common ancestor of protostomes and deuterostomes had a ventral nerve cord, as did annelids and arthropods. Within the deuterostome lineage, an axis inversion occurred, which required a shift of the mouth opening to the side opposite the nerve cord (7, 8). The second scenario assumes that the common ancestor had a diffuse nerve net that was patterned by the BMP/chordin system and coalesced ventrally in protostomes and dorsally in chordates (7, 9).

Loss of *chordin/sog* in *Drosophila* or vertebrates does not lead to the complete loss of neurogenic ectoderm, because of the presence of other mechanisms preventing BMP signaling. First, transcriptional repression of BMPs is involved. In zebrafish, the *bozozok* gene represses BMP2 expression at the dorsal side (2), whereas in *Drosophila*, the maternal Dorsal gradient ventrally represses *dpp* transcription. Second, redundant BMP antagonists play a role. In vertebrates, at least two other secreted BMP inhibitors are present: Noggin and Follistatin. Simultaneous knockdown of both inhibitors is required to observe strong phenotypes (1, 10). In *Drosophila*, target genes of BMP signaling are ventrally repressed by *brinker* (*brk*), which in turn, is dorsally repressed by BMP signaling. Only *brk sog* double mutants result in the complete loss of neurogenic ectoderm (11).

In *Drosophila*, two BMPs are involved in dorsoventral patterning: *decapentaplegic* (*dpp*), which is expressed in the dorsal 40%, and *screw* (*scw*), which is expressed along the whole embryonic circumference (12–14). Nevertheless, the highest levels of BMP signaling activity are found in a narrow dorsal stripe (15–17). The formation of this stripe depends on Sog. Sog protein is expressed in ventral cells and forms, by diffusion, a gradient, which decreases toward the dorsal side (18). Because Sog binds BMP dimers, it transports these to the dorsal side. In a broad dorsal domain, Sog is cleaved by the metalloprotease Tolloid (Tld; ref. 19). This cleavage releases the BMPs, which then can activate their receptors. The combination of these processes leads to high BMP signaling levels in a narrow dorsal stripe far away from the ventral domain of *sog* transcription (16, 19–22). Thus, the most dramatic feature of *sog* mutants is the absence of the dorsalmost cell fate, the amnioserosa (3, 5). *brinker* rescues the neurogenic ectoderm in these mutants.

The blastoderm of the short germ insect *Tribolium castaneum* has a fundamentally different architecture and does not possess a dorsal amnioserosa. The initially uniform blastoderm (Fig. 1*A*) is partitioned in an anterior extraembryonic serosa, and a more posterior germ rudiment (Fig. 1*E*). The dorsal side of this germ rudiment, as well as its anterior rim, will give rise to another extraembryonic membrane, the amnion. Furthermore, only the head and thorax segments derive from the blastodermal germ rudiment; the more posterior segments are added from a growth zone. Because *Tribolium* is thought to represent a more ancestral form of insect development (23), these differences suggest that BMP signaling underwent considerable change in the lineage leading toward *Drosophila*. To functionally compare BMP signaling in a short germ insect to *Drosophila* and vertebrates, we performed RNAi experiments with *Tc-dpp* (24) and cloned the *Tribolium sog* homologue for RNAi analysis.

Results

***Tc-sog* Is Expressed in a Ventral Domain of the Blastoderm, Whereas Tc-*dpp* Expression Initially Lacks Dorsoventral Asymmetry.** In this section, we compare the expression of *Tribolium-sog* (see Fig. 7, which is published as supporting information on the PNAS web site,

Author contributions: M.v.d.Z., O.S., and S.R. designed research; M.v.d.Z., O.S., C.v.L., and R.N.d.F. performed research; M.v.d.Z., O.S., C.v.L., R.N.d.F., and S.R. analyzed data; and M.v.d.Z. and S.R. wrote the paper.

The authors declare no conflict of interest.

This article is a PNAS direct submission.

Abbreviations: AP, anteroposterior; BMP, bone morphogenetic protein; DV, dorsoventral; IL, inner layer.

Data deposition: The sequences reported in this paper have been deposited in the GenBank database [accession nos. DQ490059 (*Tc-sog*) and DQ211693 (*Tc-doc*)].

*To whom correspondence should be addressed. E-mail: siegfried.roth@uni-koeln.de.

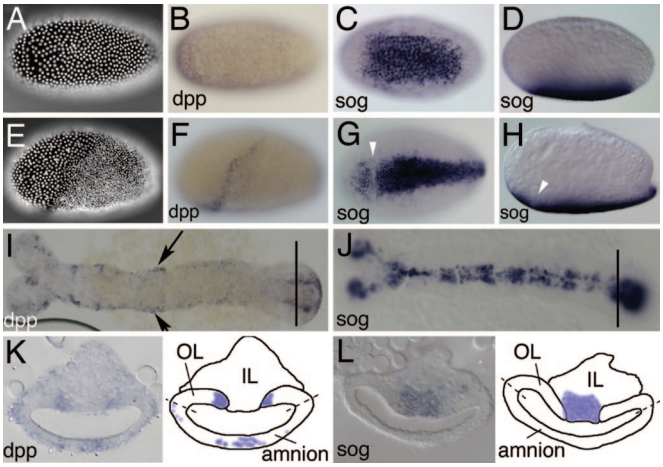

Fig. 1. Expression of *Tc-dpp* compared with expression of *Tc-sog*. (*B–D* and *F–L*) *In situ* hybridizations with *Tc-dpp* (*B*, *F*, *I*, and *K*) and *Tc-sog* (*C*, *D*, *G*, *H*, *J*, and *L*). (*A–D*) Uniform blastoderm stages. (*E–H*) Differentiated blastoderm stages. (*I* and *J*) Extending germ-band embryos. (*K* and *L*) Cross-sections from the growth zone, taken at the position of the lines in *I* and *J*, respectively. Schematic drawings are shown at *Right*. Dashed lines indicate the future border between amnion and embryo proper (*A*) DAPI counterstaining of the embryo shown in *B*. The nuclei have a uniform distribution. (*B*) Lateral view. *Tc-dpp* is ubiquitously expressed, with stronger expression at the anterior pole. (*C*) Ventral view. *Tc-sog* is expressed in a broad ventral domain. (*D*) Lateral view of the embryo shown in *C*. (*E*) DAPI counterstaining of the embryo shown in *F*. The serosa can be recognized by big, widely spaced nuclei; the germ rudiment by smaller, dense nuclei. (*F*) Lateral view. *Tc-dpp* is expressed in a stripe along the germ rudiment/serosa border. (*G*) Ventral view. The *Tc-sog* expression domain becomes narrower. A gap is observed at the germ rudiment/serosa border (white arrowhead). (*H*) Lateral view of the embryo shown in *G*. (*I*) *Tc-dpp* is expressed along the dorsal borders of the embryo (arrows), except for the growth zone. (*J*) *Tc-sog* is expressed in a ventral, ectodermal domain. Except for the growth zone, *Tc-sog* is not expressed in the mesoderm. (*K*) *Tc-dpp* is strongly expressed in two stripes in the outer layer (OL) directly flanking the IL. Weak expression is found in the amnion. (*L*) *Tc-sog* is expressed in IL cells between the OL.

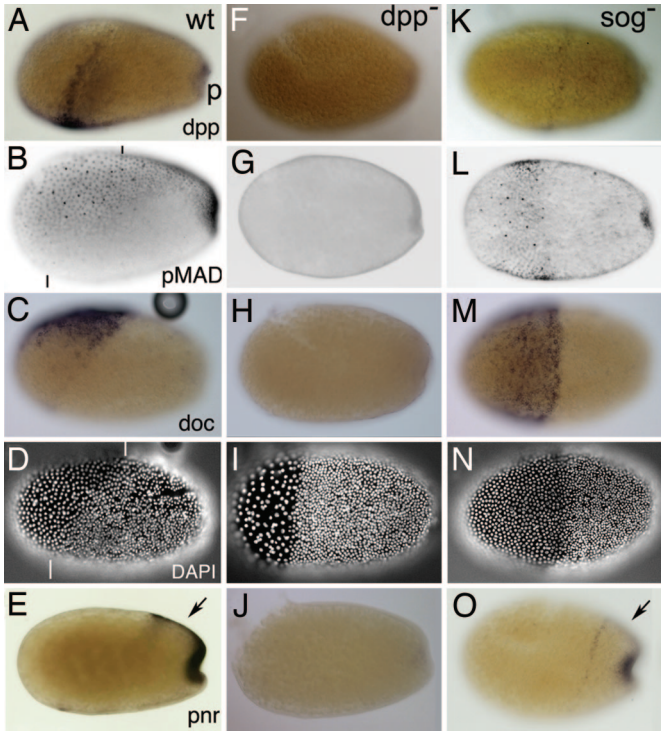

Fig. 2. Tc-Sog transports Dpp toward the dorsal side. Lateral views of embryos at the differentiated blastoderm stage. (*A–E*) Wild type (wt). (*F–J*) *Tc-dpp* RNAi (dpp^{-}). (*K–O*) *Tc-sog* RNAi (sog^{-}). (*A*, *F*, and *K*) *Tc-dpp in situ* hybridization. (*B*, *G*, and *L*) pMAD antibody staining. (*C*, *H*, and *M*) *Tc-doc in situ* hybridization. (*D*, *I*, and *N*) DAPI counterstaining of the embryos shown in *C*, *H*, and *M*, respectively. Serosal nuclei are bigger and wider spaced than those of the germ rudiment. (*E*, *J*, and *O*) *Tc-pnr in situ* hybridization. (*A*) *Tc-dpp* is expressed in a stripe along the border of the germ rudiment and serosa and in the primitive pit (p). (*B*) pMAD accumulates along the whole dorsal side of the embryo. See *Results* for details. Black lines indicate the germ rudiment/serosa border. (*C*) *Tc-doc* is transcribed in a subset of dorsal cells in the serosa. (*D*) The border of the germ rudiment and serosa is oblique (white lines indicate the dorsal and ventral point of the border). (*E*) *Tc-pnr* is expressed at the dorsal side of the germ rudiment (arrow) and in the primitive pit. (*F*) No *Tc-dpp* expression is detected. (*G*) pMAD could not be detected. (*H*) *Tc-doc* transcripts could not be detected. (*I*) The serosa/germ rudiment border is straight. (*J*) *Tc-pnr* transcripts could not be detected. (*K*) *Tc-dpp* is weakly expressed along the germ rudiment/serosa border. (*L*) pMAD is present in a band along the border of the germ rudiment and the serosa. Additional pMAD is found in the primitive pit. (*M*) *Tc-doc* is expressed in a DV symmetrical broad band in the serosa. (*N*) The germ rudiment/serosa border is straight. (*O*) *Tc-pnr* is expressed in a rim along the anterior of the germ rudiment and in the primitive pit but not at the dorsal side of the germ rudiment (arrow).

for orthology analysis) to that of *Tribolium-dpp*, the likely target of inhibition by the Tc-Sog protein. At the early, uniform blastoderm stage (Fig. 1*A*), *Tc-dpp* is expressed in all cells, with higher levels in an anterior domain (Fig. 1*B*). The pattern lacks dorsoventral (DV) asymmetry. *Tc-sog*, however, is expressed in a broad ventral domain between 20% and 80% egg length (Fig. 1 *C* and *D*). This expression domain overlaps with the area where nuclear Tc-Dorsal protein is present in *Tribolium* (25), suggesting that *Tc-sog* is a target of the maternal Tc-Dorsal gradient.

At later blastoderm stages (the differentiated blastoderm, Fig. 1*E*), *dpp* expression retracts from the anterior domain and is up-regulated at the border between serosa and germ rudiment (Fig. 1*F*). Except for its obliqueness, this stripe reflects an anteroposterior (AP) pattern rather than a DV pattern. Slightly later, *Tc-dpp* transcripts are detected in the primitive pit (Fig. 2*A*). At the differentiated germ-band stage, the *Tc-sog* domain shows a small gap at the serosa/germ rudiment border, where *Tc-dpp* is expressed (Fig. 1 *G* and *H*). Shortly thereafter, *Tc-sog* expression retracts from the presumptive serosa. The expression in the germ rudiment is slightly broader than the mesoderm at the anterior, and slightly narrower than the mesoderm at the posterior (Fig. 1*G*; ref. 26). In contrast, *Drosophila sog* expression flanks the mesoderm and never overlaps with it (6).

It is not until after gastrulation that the *Tc-sog* transcripts disappear from the invaginated mesoderm and are detected exclusively in the ventral ectoderm (Fig. 1*J*). At this stage, *Tc-dpp* is expressed in the dorsalmost ectoderm (Fig. 1*I*), clearly separated from the Tc-sog expression domain. In the growth zone, however, *Tc-sog* and *Tc-dpp* are expressed in abutting domains. *Tc-sog* is expressed in mesenchymal cells of the inner layer (IL), which is continuous with the mesoderm of the segmented region (Fig. 1*L*) (26). *Tc-dpp* is expressed in the epithelial cells of the outer layer (OL), which is continuous with the ectoderm of the segmented region (Fig. 1*K*; ref. 26). Highest *Tc-dpp* levels are found in two stripes next to the *Tc-sog* domain. Additionally, weak *Tc-dpp* expression is found in the amnion (Fig. 1*K*).

In summary, *Tc-sog* expression in the blastoderm shows a strong DV asymmetry. *Tc-dpp* expression initially lacks DV asymmetry and obtains only a slight obliqueness in the differentiated blastoderm. It is not until after gastrulation that *Tc-dpp* expression is restricted to dorsal areas (except for the growth zone).

Tc-Sog Directs Dpp Activity to the Dorsal Side. *Tc-dpp* expression at the differentiated blastoderm stage (at the border of the germ rudiment and in the primitive pit) does not correspond to the dorsal

side of the embryo (Fig. 2*A*). However, the pattern of Dpp activity strongly deviates from that of *Tc-dpp* expression. We visualized Dpp activity with antibody stainings against pMAD, the phosphorylated SMAD that is produced only in cells with activated BMP receptors (15, 27, 28). pMAD accumulates along the whole dorsal side of the embryo (Fig. 2*B*). The pMAD domain covers the dorsal 50% of the serosa and smoothly narrows toward posterior to cover the dorsal 20% in the middle of the germ rudiment. At the posterior pole, the domain broadens again. pMAD activity decreases continuously at the lateral borders of the domain, suggesting that a pMAD gradient exists.

In *Drosophila*, *pannier* (*pnr*) and *dorsocross* (*doc*) are Dpp target genes. We analyzed the expression pattern of homologs of both genes in *Tribolium* (*Tc-doc*, see *Materials and Methods*; *Tc-pnr* is TcGATAx in ref. 29). *Tc-doc* is expressed in the dorsal 30% of the serosa (Fig. 2 *C* and *D*). *Tc-pnr* marks the presumptive amnion and is expressed in the dorsal 15% of the germ rudiment and in the primitive pit (Fig. 2*E*; ref. 29). Thus, *Tc-doc* and *Tc-pnr* expression correspond to high levels of Dpp signaling in the serosa and germ rudiment, respectively.

After *Tc-dpp* RNAi (see *Materials and Methods*), 83% of the embryos lacked *Tc-dpp* expression (Fig. 2*F*) and displayed a specific phenotype ($n = 65$, analyzed for *Tc-dpp* expression). The remaining embryos were classified as WT-like but lacked detectable *Tc-dpp* transcription as well; these embryos may represent the weaker phenotypes described in ref. 30. In subsequent RNAi experiments, only embryos with strong phenotypes were analyzed. pMAD is absent after *Tc-dpp* RNAi (Fig. 2*G*), demonstrating that *Tc-dpp* is responsible for the BMP signaling activity at the dorsal side. Loss of *Tc-dpp* also abolishes *Tc-doc* and *Tc-pnr* expression (Fig. 2 *H* and *J*), confirming that both *Tc-pnr* and *Tc-doc* depend on Dpp activity, like in *Drosophila*. The absence of *Tc-pnr* indicates the loss of the amnion. In contrast to the amnioserosa in *Drosophila*, however, the *Tribolium* serosa still forms in absence of BMP signaling, although its border with the germ rudiment is no longer oblique, but becomes straight (Fig. 2*I*, compare with 2*D*).

The spatial discrepancy between *Tc-dpp* expression and Dpp activity in the WT might be explained by assuming that ventrally produced Sog molecules transport Dpp toward the dorsal side, like in *Drosophila*. To test this hypothesis, *Tc-dpp* expression and pMAD distribution were analyzed in *Tc-sog* RNAi embryos. *Tc-sog* RNAi knocked down *Tc-sog* transcription in all embryos and led in 97% of the cases to a specific phenotype ($n = 57$ embryos analyzed for *Tc-sog* expression). Subsequent *Tc-sog* RNAi experiments revealed that *Tc-dpp* expression retracts from an anterior domain to a rim between the serosa and germ rudiment, similar to the WT (Fig. 2*K*). However, the border between serosa and germ rudiment is straight also after *Tc-sog* RNAi (Fig. 2*N*). Accordingly, the stripe of *Tc-dpp* expression is symmetric along the DV axis, indicating that the obliqueness of *Tc-dpp* expression itself depends on Sog.

In *Tc-sog* RNAi embryos, pMAD is not present in a dorsal domain, but in a broad, vertical band overlapping the stripe of *dpp* expression (Fig. 2*L*). This shift shows that the dorsal localization of Dpp activity depends on Sog. Unaided diffusion of Dpp molecules might cause the band of BMP activity to be broader than the stripe of *Tc-dpp* expression (22, 31). The expression domains of the Dpp target genes, *Tc-doc* and *Tc-pnr*, lose their dorsal localization as well. *Tc-doc* expression shifts from a dorsal domain to a broad DV-symmetric band of expression within the serosa, overlapping the pMad domain (Fig. 2*M*). The dorsal *Tc-pnr* domain is also lost (Fig. 2*O*, arrow). *Tc-pnr* rather follows the *Tc-dpp* expression and is expressed in a rim along the border of germ rudiment and serosa and in the primitive pit (Fig. 2*O*). *Tc-doc* and *Tc-pnr* expression show that serosal and some amniotic tissue still is present after *Tc-sog* RNAi. However, these tissues obtain positions along the AP axis.

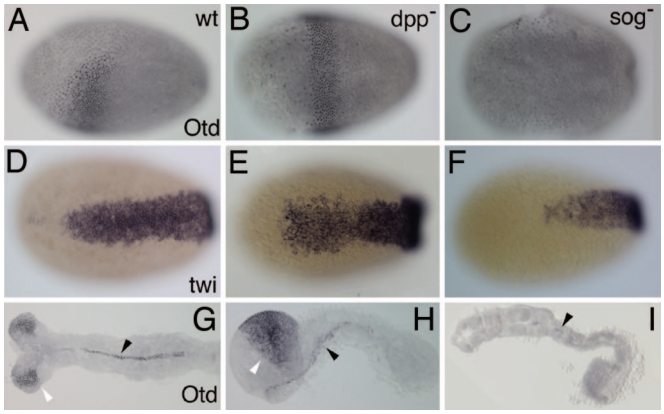

Fig. 3. *Tc-sog* RNAi deletes the head; *Tc-dpp* RNAi enlarges the head. (*A–F*) Differentiated blastoderm stages. (*A–C*) Tc-Otd antibody stainings, lateral views. (*D–F*) *Tc-twist in situ* hybridizations, differentiated blastoderm stages, ventral views. (*G–I*) Tc-Otd antibody stainings; extended germ-band embryos. (*A*) WT. Tc-Otd is present in an anterior triangle. (*B*) *Tc-dpp* RNAi. Tc-Otd is present in a band in the anterior germ rudiment. (*C*) *Tc-sog* RNAi. Tc-Otd could not be detected. (*D*) WT. (*E*) *Tc-dpp* RNAi. The *Tc-twist* domain extends to a WT position along the AP axis but is slightly broader in the anterior half. (*F*) *Tc-sog* RNAi. The *Tc-twi* domain is only half as long as in the WT. (*G*) WT. Tc-Otd is found in the head lobes (open arrowhead) and along the ventral midline (filled arrowhead). (*H*) *Tc-dpp* RNAi, lateral view. Tc-Otd is detected along the ventral midline (filled arrowhead) and in an enlarged anterior domain (open arrowhead). (*I*) *Tc-sog* RNAi. Tc-Otd is detected only in some patches along the ventral midline (arrowhead).

Most importantly, the coincidence of *Tc-dpp* expression and Dpp activity after *Tc-sog* RNAi strongly suggests that, in WT, concentration-driven ventral-to-dorsal transport by Tc-Sog enriches Dpp molecules at the dorsal side.

BMP Signaling Plays a Role in Head Formation in *Tribolium*. The straight serosa/germ rudiment border after *Tc-dpp* and *Tc-sog* RNAi has far reaching consequences for AP patterning. In WT, the border of the germ rudiment and serosa is oblique and runs from a dorsal, more posterior position to a ventral, more anterior position (Fig. 2*D*). Accordingly, the anterior part of the germ rudiment can be described as a triangle. The head gap gene *Tc-orthodenticle* (*Tc-otd*) is expressed within this triangle (Fig. 3*A*; ref. 32). After *Tc-dpp* RNAi, the germ rudiment/serosa border is straight and is located at the more anterior (ventral) position (Fig. 2*I*). As a result, the Tc-Otd domain expands toward the dorsal side and forms a broad dorsoventrally symmetric ring at the anterior germ rudiment (Fig. 3*B*). After *Tc-sog* RNAi, the germ rudiment/serosa border is straight as well but is located at the more posterior (dorsal) position (Fig. 2*N*). Consequently, the Tc-Otd domain is lost after *Tc-sog* RNAi (Fig. 3*C*). BMP signaling also influences the anterior mesoderm. *Tc-dpp* RNAi enlarges this tissue, whereas *Tc-sog* RNAi completely deletes it, as revealed by morphological analyses and *Tc-twist* stainings (Fig. 3 *D–F*). On the contrary, *Drosophila twist* is only under control of maternal Dorsal and is insensitive to changes in BMP signaling.

In the extending germ band (gastrulation is described in detail in the *Supporting Results*, which is published as supporting information on the PNAS web site), Tc-Otd is present in the head lobes (Fig. 3*G*). Additional Otd can be detected along the ventral midline (Fig. 3*G*). After *Tc-dpp* RNAi, Tc-Otd reveals strikingly enlarged headlobes (Fig. 3*H*). In contrast, anterior Tc-Otd is completely absent after *Tc-sog* RNAi (Fig. 3*I*). Similar results are obtained when the anterior domain of the newly described segmentation gene *milles pattes* (*Tc-mlpt*; ref. 33) is

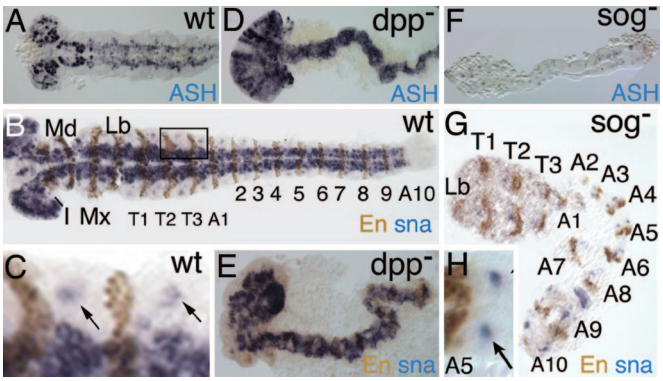

Fig. 4. *Tc-sog* RNAi leads to a complete loss of the neurogenic ectoderm; extending germ-band embryos. (*A–C*) WT. (*D* and *E*) *Tc-dpp* RNAi. (*F–H*) *Tc-sog* RNAi. (*A*, *D*, and *F*) *Tc-achaete-scute in situ* hybridizations. (*B–H*) *Tc-snail in situ* hybridizations (blue) with engrailed antibody staining (brown). (*A*) *Tc-ASH* is expressed in cells of the CNS and in a transverse stripe at the anterior of each segment. (*B*) *Tc-snail* is expressed in cells of the CNS. Seventeen engrailed stripes could be counted. Segments are labeled as follows: I, intercallary; Md, mandibular; Mx, maxillary; Lb, labial; T, thoracic; A, abdominal. (*C*) Magnification of a part of the embryo boxed in *B*. *Tc-snail* is also detected in single clusters marking the peripheral neurons of the lateral ectoderm (arrows). (*D*) *Tc-ASH* transcripts can be detected throughout the embryo. (*E*) *Tc-snail* can be detected throughout the embryo. (*F*) *Tc-ASH* can be detected only in segmental stripes. (*G*) *Tc-snail* expression is found only in single clusters. Only 13 engrailed stripes were counted. (*H*) Magnification of segment A5 from the embryo shown in *E*. The arrow points at the peripheral neurons.

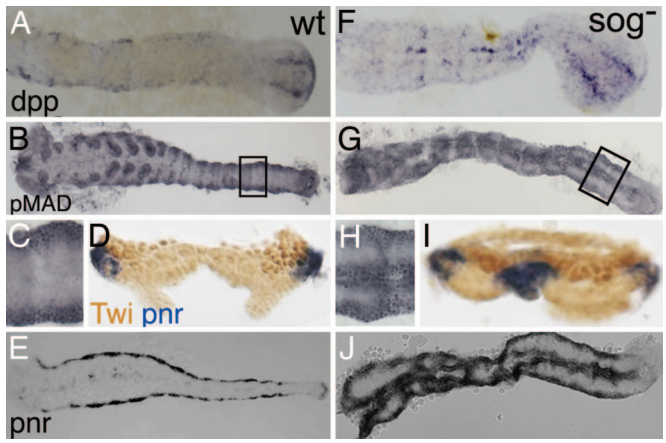

Fig. 5. *Tc-sog* RNAi embryos show a double dorsal phenotype. (*A–E*) WT. (*F–J*) *Tc-sog* RNAi. (*A* and *F*) *Tc-dpp in situ* hybridizations. (*B*, *C*, *G*, and *H*) pMAD antibody staining. (*D* and *I*) Cross-sections with *Tc-pnr in situ* hybridization (blue) and Twist antibody staining marking the mesoderm (dark brown). (*E* and *J*) *Tc-pnr in situ* hybridizations. (*A*) *Tc-dpp* is expressed along the dorsal borders of the extending germ band and in two stripes in the growth zone. (*B*) pMAD is detected along the dorsal margins of the extended germ band. (*C*) Magnification of the area boxed in *B*. (*D* and *E*) *Tc-pnr* is expressed at the dorsal margins. (*F*) *Tc-dpp* is weakly expressed along the dorsal margins and in two strong ectopic stripes along the ventral midline. The stripes are continuous, with the stripes in the growth zone. (*G*) pMAD is detected along the dorsal margins of the germ band and in a strong ectopic domain along the ventral midline. (*H*) Magnification of the area boxed in *D*. (*I* and *J*) *Tc-pnr* is expressed along the dorsal margin and in a strong, ventral, ectopic stripe in the ectoderm.

used as a marker for the head region (Fig. 8, which is published as supporting information on the PNAS web site).

To investigate the number and identity of the deleted anterior segments, we analyzed the expression of anterior Hox genes (*Tc-Antennapedia*, *Tc-Sex combs reduced*, and *Tc-Deformed*) in *Tc-sog* RNAi embryos (Fig. 9, which is published as supporting information on the PNAS web site). These experiments revealed that, anterior to the thorax, only one reduced segment is present that has a labial identity. This finding was corroborated by analysis of the cuticles (Fig. 10 *D* and *E*, which is published as supporting information on the PNAS web site). Analysis of engrailed stripes (Fig. 4 *B* and *G*) confirmed that, instead of the 17 WT engrailed stripes (Fig. 4*B*), only 13 engrailed stripes plus a small patch of engrailed expression were present, corresponding to the 10 abdominal, 3 thoracic, and 1 reduced segment (Fig. 4*G*). Taken together, BMP signaling has to be inhibited by *sog* to allow head formation in *Tribolium*. In contrast, the presence of *Dm-otd* expression in dorsalized embryos indicates that BMP signaling does not influence the number of head segments in *Drosophila* (Fig. 11, which is published as supporting information on the PNAS web site).

***Tc-dpp* RNAi Enlarges and *Tc-sog* RNAi Completely Deletes the Neurectoderm.** To assess the effect of *Tc-dpp* or *Tc-sog* RNAi on neurogenesis, embryos were stained with *Tc-achaete-scute* (*Tc-ASH*; ref. 34) and *Tc-snail* (35) at the extended germ-band stage. In WT, *Tc-ASH* is expressed in cells of the CNS plus in an anterior ectodermal stripe in each segment (Fig. 4*A*; ref. 34). *Tc-snail* is expressed in the CNS as well (Fig. 4*B*) and, additionally, in neurons of the peripheral nervous system, which mark the lateral (nonneurogenic) ectoderm (Fig. 4*C*). *Tc-dpp* RNAi embryos consist only of neurogenic ectoderm, because *Tc-ASH* and *Tc-snail* expression is found throughout the embryonic circumference (Fig. 4 *D* and *E*). In contrast, only the segmental stripes of *Tc-ASH* could be detected after *Tc-sog* RNAi (Fig. 4*F*). Similarly, *Tc-snail* expression was found only in single clusters of cells, the peripheral neurons (Fig. 4 *G* and *H*). Thus, the loss of *Tc-sog* causes a deletion of the entire CNS. This phenotype is stronger than that of *sog* in *Drosophila* or *chordin* in vertebrates.

***Tc-sog* RNAi Leads to a "Double Dorsal" Phenotype.** To investigate the effect of altered BMP signaling on the dorsal ectoderm, *Tc-dpp* expression, MAD phosphorylation, and *Tc-pnr* expression were investigated at the extended germ-band stage. At this stage, *Tc-pnr* does not mark only the amnion but is additionally expressed along the dorsal margins of the germ band and marks the dorsal ectoderm (ref. 36; Fig. 5 *D* and *E*). The stripes of *Tc-pnr* expression correspond to the dorsal *Tc-dpp* expression and high pMAD levels (Fig. 5 *A–C*). In *Tc-dpp* RNAi embryos, *Tc-dpp* expression, MAD phosphorylation, and *Tc-pnr* expression were completely abolished (data not shown), confirming the assumption that *Tc-dpp* RNAi embryos possess only ventral (neurogenic) ectoderm.

Surprisingly, dorsal pMAD staining is not expanded in *Tc-sog* RNAi embryos but is found in an additional, ectopic domain in the ectoderm at each side of the ventral midline (Fig. 5 *G* and *H*). This ectopic domain coincides with two stripes of ectopic *Tc-dpp* expression along the ventral midline (Fig. 5*F*). *Tc-pnr* follows the pattern of Tc-Dpp activity and is ectopically expressed in a ventral, ectodermal stripe, in addition to the dorsal expression (Fig. 5 *I* and *J*). Because the peripheral neurons detected with *Tc-snail* lie between the two *Tc-pnr* expression domains, we assume that lateral ectoderm is present between the stripes of dorsal ectoderm. This double dorsal phenotype is confirmed by the analysis of cuticular markers (see *Supporting Results* and Fig. 10).

The two stripes of ectopic *Tc-dpp* expression in *Tc-sog* RNAi embryos are continuous with the *Tc-dpp* expression stripes of the growth zone (Fig. 5*F*). This expression pattern suggests that in absence of *Tc-sog*, a growth zone-specific pattern persists that prevents the establishment of correct DV polarity within the ectoderm of the newly emerging segments.

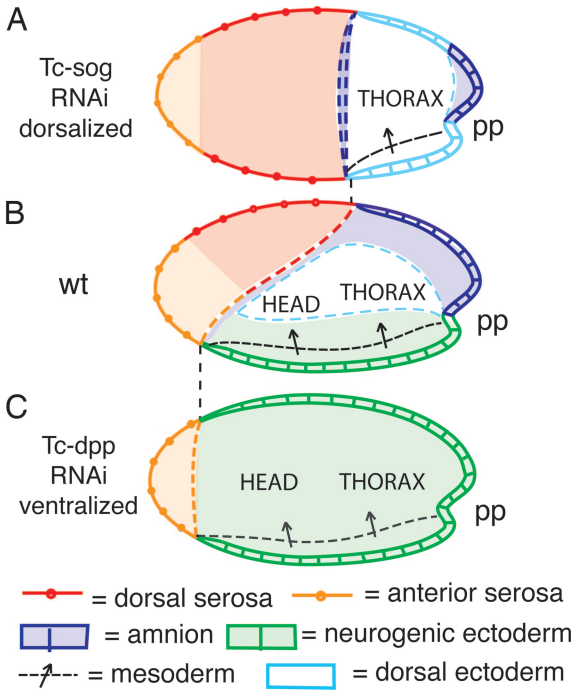

Fig. 6. Schematic drawings of the *Tc-sog* and *Tc-dpp* RNAi phenotypes. (*A*) *Tc-sog* RNAi. The neurogenic ectoderm (green) is absent. Dorsal cell fates occupy domains along the AP axis: Dorsal serosal cells (red) are present in a broad band anterior to the germ rudiment, and amniotic cells (dark blue) are present along the anterior margin of the germ rudiment and in the primitive pit. Dorsal amnion is absent. The serosa/germ rudiment border is straight and is located at the position of the dorsal border in WT. The presumptive mesoderm (dotted line with arrow) is correspondingly shorter along the AP axis. (*B*) WT. Dorsal serosal cells and amniotic cells are localized to the dorsal side. Neurogenic ectoderm and mesoderm are present. The germ rudiment/serosa border is oblique and runs from a dorsal, posterior position to a ventral, anterior position. (*C*) *Tc-dpp* RNAi. Dorsal serosa and amnion are absent. Mesoderm and an anterior serosa (orange) are present. The germ rudiment/serosa border is straight and located at the position of the WT ventral border. The rest of the embryo consists of neurogenic ectoderm. pp, primitive pit.

Discussion

The Role of Dpp Transport by Sog. One of the main findings of this study is that Sog-mediated Dpp transport imposes DV polarity on BMP signaling in *Tribolium*. After *Tc-sog* knockdown, *Tc-dpp* expression, Dpp activity, and Dpp target genes acquire dorsoventrally symmetric domains along the AP axis (Fig. 6). The first morphologically visible sign of DV polarity, the obliqueness of the border between serosa and germ rudiment, also is lost. This border becomes straight, implying that the distinction between serosa and germ rudiment is primarily set up by inputs from the AP system and secondarily modulated through BMP signaling. We suggest that target genes exist that are involved in serosa specification (a likely candidate is *zerknüllt 1*; ref. 29) and which sense both an AP gradient (of unknown nature) and the DV gradient of BMP activity established by Sog. This combinatorial input would lead to tilted expression domains, establishing the oblique border between serosa and germ rudiment. In turn, *Tc-dpp* itself becomes up-regulated along this border. This obliqueness is the earliest DV asymmetry in the initially DV symmetric expression of *Tc-dpp*.

This situation is clearly different from *Drosophila*. There, the maternal NFκB/Dorsal gradient already imposes a DV prepattern on the embryo by repressing *Dm-zen* and *Dm-dpp* at the ventral side (13). The dorsal stripe of highest Dpp activity does not require a complete redistribution of Dpp molecules from their site of expression by Sog. However, the *Drosophila* system also has the capability to generate a dorsal stripe of Dpp activity independently from the pattern of *Dm-dpp* expression. When *Dm-dpp* is artificially expressed under the control of the *even-skipped* stripe 2 enhancer (in a *Dm-dpp* minus background), Sog-dependent transport still correctly localizes Dpp activity to a dorsal stripe (22). In *Tribolium*, the stripe of *Tc-dpp* expression between serosa and germ rudiment appears to be the major source for Dpp protein transported to the dorsal side. Thus, the formation of the dorsal Dpp activity domain in the *Tribolium* embryo has similarity to the experimental conditions in *Drosophila*, where *Dm-dpp* is expressed in the *even-skipped* stripe.

In *Drosophila*, the transport mechanism establishes a sharply demarcated stripe of high level Dpp/Scw signaling. In contrast, in *Tribolium*, the transport mechanism establishes a BMP-signaling domain with smooth borders. The accuracy in *Drosophila* might depend on the presence of *scw*, because the formation of Scw-Dpp heterodimers has been shown to contribute to the robustness of the patterning output (16). A *scw* homologue was not found in the *Tribolium* genome (M.v.d.Z., R.N.d.F., and S.R., unpublished results). In addition, in *Drosophila*, a positive feedback circuitry promoting future ligand binding as a function of previous signaling strength is required to generate the sharply demarcated stripe of high BMP signaling (22, 31). This feedback circuitry might be absent in *Tribolium*. Robust and accurate dorsal localization of Dpp activity was probably crucial for the evolution of long-germ development, because in long-germ insects, the extraembryonic membrane derives only from the dorsalmost side of the blastoderm. Absence of the amnioserosa in *Dm-sog* mutants causes a severe disruption of morphogenetic movements. In the absence of *sog* in *Tribolium*, however, serosal and amniotic tissue still derive from positions along the AP axis (Figs. 2*O* and 6*A*), allowing rather normal morphogenetic movements (*Supporting Results* and Figs. 12 and 13, which are published as supporting information on the PNAS web site).

The Function of Sog in the Growth Zone and the Origin of the Double Dorsal Phenotype. *Tc-sog* RNAi completely deletes the neurogenic ectoderm and causes a double dorsal phenotype with ectopic dorsal ectoderm along the ventral midline. The origin of the specification of this ectopic dorsal ectoderm might lie in the expression pattern of *Tc-dpp* in the growth zone. Besides a weak expression in the amnion, *Tc-dpp* is expressed in two strong stripes directly flanking the IL of the growth zone (Fig. 1*K*). An inherent positive feedback mechanism of Dpp signaling on *Tc-dpp* transcription might tend to maintain this transcription at the border with the mesoderm (i.e., at the ventral side). In WT, *Tc-sog* is expressed in the IL and might block Dpp signaling in the neighboring ventral outer layer (OL), thus preventing feedback. Indeed, the inner stripes of *Tc-dpp* disappear during segment formation in the WT. In absence of Tc-Sog, however, these inner stripes are maintained.

We have even indications that Tc-Sog is involved in establishing the dorsal domain of *Tc-dpp* transcription during segment formation, because a few *Tc-sog* RNAi embryos completely lacked the dorsal *Tc-dpp* expression and contained only the ventral stripes. Because this phenotype was observed in only a small minority of the embryos, it is likely that additional, yet unidentified components play a role in establishing the correct polarity of BMP signaling during segment formation in the growth zone.

Comparisons with Vertebrates and the Function of BMP Signaling in Head Formation. A BMP transport mechanism by BMP antagonists is present not only in *Tribolium* and *Drosophila*, but is also believed to exist in some vertebrates. In zebrafish, the ventralmost cell fate, the ventral tail fin, is absent in *chordin* mutants (2). However, it appears that the enrichment of BMP activity by chordin-mediated BMP transport is less important in vertebrates. Thus, it is possible that a transport mechanism was present in the ancestor of insects and vertebrates and only in insects did it acquire a major role.

A feature in which *Drosophila* and vertebrates differ from *Tribolium* is the presence of redundancy. In *Tribolium*, Tc-Sog is the main inhibitor of BMPs, because its loss leads to the complete absence of neurogenic tissue. In contrast, *Drosophila brinker* rescues the neurogenic ectoderm in *Dm-sog* mutants. The *Tribolium brinker* gene appears not to be expressed in the embryo (R.N.d.F. and S.R., unpublished results). In vertebrates, redundant excreted BMP antagonists like Noggin prevent the loss of neuronal tissue in *chordin* mutants. No Noggin homologue was found in the available *Tribolium* genome sequence. It is plausible that the different types of redundancy independently evolved from a common, simple mechanism. Because *chordin/sog* is common to all systems and because Tc-Sog is the main BMP inhibitor in *Tribolium*, we suggest that a common ancestor of vertebrates and insects possessed a BMP-signaling system in which Sog/Chordin is the sole BMP antagonist. Consistently, in a spider, *sog* also is the main BMP inhibitor, and its loss leads to the complete absence of the CNS (37).

In vertebrates, BMP signaling plays an important role in the development of the head. Depletion of chordin and other BMP antagonists results in reduction of head and forebrain (e.g., refs. 10 and 38 for mouse), whereas BMP knockdown enlarges the head and forebrain (ref. 39 for *Xenopus*). The most surprising finding of this study is a similar effect of BMP signaling on *Tribolium* head formation. *Tc-dpp* RNAi enlarges the headlobes and anterior mesoderm, whereas *Tc-sog* RNAi deletes the headlobes, anterior mesoderm, and three cephalic segments. On the contrary, BMP signaling does not play a role in head specification in *Drosophila* (Fig. 11). It could be that BMP signaling was independently coopted for head formation in *Tribolium*. However, *Tribolium* might be more representative for arthropod head development than *Drosophila*, because the *Drosophila* head is specified in an exceptional way involving the maternal *bicoid* gene, which is present only in a group of derived Diptera (40). Therefore, the input of BMPs on anterior patterning might have been lost in *Drosophila*, and the similarity between *Tribolium* and vertebrates might reflect an ancestral involvement of BMP signaling in head formation. Interestingly, *chordin/sog* of a cnidarian shows a strong asymmetry along the AP axis and is expressed at the blastoporal pole (41, 42), which is thought to correspond to the anterior pole of Bilateria (43). However, more invertebrates should be investigated to fully resolve this question.

Materials and Methods

Stock keeping, embryo fixation, synthesis of dsRNA, *in situ* hybridizations, immunostainings, and cuticle preparation were performed as described in ref. 29. Araldite sections were performed as described in ref. 44.

Cloning of *Tc-sog* and *Tc-doc*. A Tc-sog fragment was obtained by a seminested PCR with the degenerate primers reverse1, ACDATIGCIGTICCICCIGCICC (recognizing GAGGTAIV); forward1, AAYCCICARAAYGTIGTIGC (recognizing NPQNVVA); and forward2, CCICARAAYGTIGTIGCIAC (recognizing PQNVVAT), whereas *Tc-doc* was found *in silico* on the basis of the available genome sequence (www.hgsc.bcm.tmc.edu/projects/tribolium) and was cloned with the specific primers ATCCGCCGACTACTGCCTCTTCCT and CTAACTGTTTCCGCTTCGCACTCG. Sequences were completed by RACE (BD Biosciences, San Jose, CA).

Parental RNAi. Because pupal *Tc-dpp* RNAi interfered with female maturation and resulted in sterility, all dsRNA injections were performed in adult beetles. Mature, female beetles were cooled on ice for 2 min and were ventrally fixed on a microscope slide with double-sided tape. One elytrum was lifted, and 0.1 μl of a 0.5–1.0 μg/μl dsRNA solution was dorsally injected. The females were released immediately from the tape and allowed to recover for one night before males were added. Eggs were collected 1–3 days thereafter.

We thank Luis Saraiva for help with the cloning of *Tc-doc*, Abidin Basal for help with the double stainings, Reinard Schröder (University of Tübingen, Tübingen, Germany) for the Tc-Otd antibody, Alfonso Martinez-Arias (University of Cambridge, Cambridge, U.K.) for an aliquot of the pMAD antibody, Scott Wheeler and James Skeath (both from Washington University School of Medicine, St. Louis, MO) for the Tc-ASH plasmid, and Jeremy Lynch for helpful comments on the manuscript. M.v.d.Z., C.v.L., and R.N.d.F. were funded by the International Graduate School in Genetics and Functional Genomics of the University of Cologne and the SFB 680.

1. De Robertis EM, Kuroda H (2004) *Annu Rev Cell Dev Biol* 20:285–308.
2. Hammerschmidt M, Mullins MC (2002) *Results Probl Cell Differ* 40:72–95.
3. Ferguson EL, Anderson KV (1992) *Cell* 71:451–461.
4. Wharton KA, Ray RP, Gelbart WM (1993) *Development (Cambridge, UK)* 117:807–822.
5. Biehs B, Francois V, Bier E (1996) *Genes Dev* 10:2922–2934.
6. Francois V, Solloway M, O'Neill JW, Emery J, Bier E (1994) *Genes Dev* 8:2602–2616.
7. Gerhart J (2000) *Proc Natl Acad Sci USA* 97:4445–4448.
8. Arendt D, Nubler-Jung K (1994) *Nature* 371:26.
9. Lowe CJ, Wu M, Salic A, Evans L, Lander E, Stange-Thomann N, Gruber CE, Gerhart J, Kirschner M (2003) *Cell* 113:853–865.
10. Bachiller D, Klingensmith J, Kemp C, Belo JA, Anderson RM, May SR, McMahon JA, McMahon AP, Harland RM, Rossant J, De Robertis EM (2000) *Nature* 403:658–661.
11. Jazwinska A, Rushlow C, Roth S (1999) *Development (Cambridge, UK)* 126:3323–3334.
12. Arora K, Levine MS, O'Connor MB (1994) *Genes Dev* 8:2588–2601.
13. Ray RP, Arora K, Nusslein-Volhard C, Gelbart WM (1991) *Development (Cambridge, UK)* 113:35–54.
14. St Johnston RD, Gelbart WM (1987) *EMBO J* 6:2785–2791.
15. Dorfman R, Shilo BZ (2001) *Development (Cambridge, UK)* 128:965–972.
16. Shimmi O, Umulis D, Othmer H, O'Connor MB (2005) *Cell* 120:873–886.
17. Sutherland DJ, Li M, Liu XQ, Stefancsik R, Raftery LA (2003) *Development (Cambridge, UK)* 130:5705–5716.
18. Srinivasan S, Rashka KE, Bier E (2002) *Dev Cell* 2:91–101.
19. Marques G, Musacchio M, Shimell MJ, Wunnenberg-Stapleton K, Cho KW, O'Connor MB (1997) *Cell* 91:417–426.
20. Ashe HL, Levine M (1999) *Nature* 398:427–431.
21. Eldar A, Dorfman R, Weiss D, Ashe H, Shilo BZ, Barkai N (2002) *Nature* 419:304–308.
22. Wang YC, Ferguson EL (2005) *Nature* 434:229–234.
23. Roth S (2004) in *Gastrulation: From Cells to Embryos*, ed Stern C (Cold Spring Harbor Lab Press, Plainview, NY), pp 105–121.
24. Sanchez-Salazar J, Pletcher MT, Bennett RL, Brown S, Dandamudi TJ, Denell R, Doctor JS (1996) *Dev Genes Evol* 206:237–246.
25. Chen G, Handel K, Roth S (2000) *Development (Cambridge, UK)* 127:5145–5156.
26. Handel K, Basal A, Fan X, Roth S (2005) *Dev Genes Evol* 215:13–31.
27. Persson U, Izumi H, Souchelnytskyi S, Itoh S, Grimsby S, Engstrom U, Heldin CH, Funa K, ten Dijke P (1998) *FEBS Lett* 434:83–87.
28. Tanimoto H, Itoh S, ten Dijke P, Tabata T (2000) *Mol Cell* 5:59–71.
29. van der Zee M, Berns N, Roth S (2005) *Curr Biol* 15:624–636.
30. Ober KA, Jockusch EL (2006) *Dev Biol.* 294:391–405.
31. Mizutani CM, Nie Q, Wan FY, Zhang YT, Vilmos P, Sousa-Neves R, Bier E, Marsh JL, Lander AD (2005) *Dev Cell* 8:915–924.
32. Li Y, Brown SJ, Hausdorf B, Tautz D, Denell RE, Finkelstein R (1996) *Dev Genes Evol* 206:35–45.
33. Savard J, Marques-Souza H, Aranda M, Tautz D (2006) *Cell* 126:559–569.
34. Wheeler SR, Carrico ML, Wilson BA, Brown SJ, Skeath JB (2003) *Development (Cambridge, UK)* 130:4373–4381.
35. Sommer RJ, Tautz D (1994) *Dev Genet* 15:32–37.
36. Berns N (2001) Dissertation (University of Cologne, Cologne, Germany).
37. Akiyama-Oda Y, Oda H (2006) *Development (Cambridge, UK)* 133:2347–2357.
38. Anderson RM, Lawrence AR, Stottmann RW, Bachiller D, Klingensmith J (2002) *Development (Cambridge, UK)* 129:4975–4987.
39. Reversade B, Kuroda H, Lee H, Mays A, De Robertis EM (2005) *Development (Cambridge, UK)* 132:3381–3392.
40. Stauber M, Prell A, Schmidt-Ott U (2002) *Proc Natl Acad Sci USA* 99:274–279.
41. Matus DQ, Thomsen GH, Martindale MQ (2006) *Curr Biol* 16:499–505.
42. Rentzsch F, Anton R, Saina M, Hammerschmidt M, Holstein TW, Technau U (2006) *Dev Biol* 296:375–387.
43. Martindale MQ (2005) *Nat Rev Genet* 6:917–927.
44. Roth S, Stein D, Nusslein-Volhard C (1989) *Cell* 59:1189–1202.